


# Modelling and commissioning validation of eclipse conical cone collimator for stereotactic radiosurgery using Monte Carlo simulation

Ravindra Shende<sup>1,2</sup> , S. J. Dhoble<sup>2</sup>, Dinesh Saroj<sup>1</sup> and Gourav Gupta<sup>1</sup>

<sup>1</sup>Department of Radiation Oncology, Balco Medical Centre, New Raipur, Chhattisgarh, India and <sup>2</sup>Department of Physics, Rashtrasant Tukadoji Maharaj Nagpur University, Nagpur, Maharashtra, India

## Original Article

**Cite this article:** Shende R, Dhoble SJ, Saroj D, and Gupta G. (2024) Modelling and commissioning validation of eclipse conical cone collimator for stereotactic radiosurgery using Monte Carlo simulation. *Journal of Radiotherapy in Practice*. **23**(e7), 1–12. doi: [10.1017/S1460396924000025](https://doi.org/10.1017/S1460396924000025)

Received: 23 August 2023  
Revised: 20 December 2023  
Accepted: 11 January 2024

### Keywords:

commissioning validation; conical cone; Monte Carlo; PRIMO; SRS

### Corresponding author:

Ravindra Shende;  
Email: [ravindrashende02@gmail.com](mailto:ravindrashende02@gmail.com)

## Abstract

**Purpose:** The miniaturized conical cones for stereotactic radiosurgery (SRS) make it challenging in measurement of dosimetric data needed for commissioning of treatment planning system. This study aims at validating dosimetric characteristics of conical cone collimator manufactured by Varian using Monte Carlo (MC) simulation technique.

**Methods & Material:** Percentage depth dose (PDD), tissue maximum ratio (TMR), lateral dose profile (LDP) and output factor (OF) were measured for cones with diameters of 5mm, 7.5mm, 10mm, 12.5 mm, 15 mm and 17.5 mm using EDGE detector for 6MV flattening filter-free (FFF) beam from Truebeam linac. Similarly, MC modelling of linac for 6MVFFF beam and simulation of conical cones were performed in PRIMO. Subsequently, measured beam data were validated by comparing them with results obtained from MC simulation.

**Results:** The measured and MC-simulated PDDs or TMRs showed close agreement within 3% except for cone of 5mm diameter. Deviations between measured and simulated PDDs or TMRs were substantially higher for 5mm cone. The maximum deviations at depth of 10cm, 20cm and at range of 50% dose were found 4.05%, 7.52%, 5.52% for PDD and 4.04%, 7.03%, 5.23% for TMR with 5mm cone, respectively. The measured LDPs acquired for all the cones showed close agreement with MC LDPs except in penumbra region around 80% and 20% dose profile. Measured and MC full-width half maxima of dose profiles agreed with nominal cone size within  $\pm 0.2$  mm. Measured and MC OFs showed excellent agreement for cone sizes  $\geq 10$  mm. However, deviation consistently increases as the size of the cone gets smaller.

**Findings:** MC model of conical cones for SRS has been presented and validated. Very good agreement was found between experimentally measured and MC-simulated data. The dosimetry dataset obtained in this study validated using MC model may be used to benchmark beam data measured for commissioning of SRS for cone planning.

## Introduction

The greater dosimetric accuracy and geometrical precision are required to deliver a very high dose of radiation during stereotactic radiosurgery (SRS). The conical cone collimator (CCC) is a tertiary collimator that usually provides a small circular opening of 4 mm to 20 mm diameter defined at the isocentre. CCC has become predominantly used for SRS in the treatment of brain tumours like arteriovenous malformation, trigeminal neuralgia, acoustic neuroma and pituitary tumours.<sup>1,2</sup> CCC offers a smaller penumbra, sharper dose fall-off, higher mechanical stability and lower transmission than multi-leaf collimator (MLC). However, small-field radiation dosimetry is itself challenging due to the lack of electronic equilibrium, detector size, steep dose gradient, partial volume averaging effect and occlusion of the radiation source. Besides this, the beam data required for the commissioning of SRS cone demand higher dosimetric and geometrical accuracy. Several studies have reported 10% uncertainty in the measurement of small-field dosimetric data below 10 mm.<sup>3</sup> The most critical parameter is the output factor (OF) which is very sensitive to field size, detector type and positioning of the detector.<sup>3,4</sup> The independent validation of these experimental data is essential during the commissioning of CCC for SRS before clinical use.

The techniques of Monte Carlo (MC) are well-established in the field of medical radiation physics. The MC techniques are recognized as the most accurate ways for predicting the dose during radiation transport with minimum uncertainties.<sup>5</sup> CCC offers a small circular field that has difficulties in establishing electronic equilibrium where larger dosimetric uncertainties are involved. The MC technique is well known for obtaining an accurate dose distribution in a small field by accounting for the loss of electronic equilibrium, dose from buildup region and backscatter. MC has been widely used for the commissioning and clinical validation of photon and electron beams. The MC simulation technique provides an independent and highly accurate way of predicting absorbed dose distribution in diverse geometries. Numerous studies have

© The Author(s), 2024. Published by Cambridge University Press. This is an Open Access article, distributed under the terms of the Creative Commons Attribution licence (<http://creativecommons.org/licenses/by/4.0/>), which permits unrestricted re-use, distribution and reproduction, provided the original article is properly cited.

availed the MC simulation technique for dosimetric evaluation of CCC from different vendors.<sup>6–9</sup> The works published by Cheng et al.<sup>6</sup> are the well-known set of data published related to the dosimetry of the SRS cone for 6MV flattening filter-free (FFF) beam from Varian. However, Cheng et al. work is limited to the comparison of simulated and measured output cone factors.

There have been many publications reporting experimental data on the SRS commissioning of different medical linear accelerators (Linac) with micro MLC and CCC.<sup>10–14</sup> However, there is a wide variety of available literature that is very much diversified and differentiated based on different aspects of SRS commissioning. This makes it very difficult to establish comparisons between the present set of data. The authors Gocha Khelashvili et al. (2011), Marcelino Hermida-Lopez et al. (2012) and Wiant D B et al. (2013)<sup>10,14,15</sup> reported most of the experimental data on SRS commissioning using the Brain lab stereotactic cone. However, very limited literature is available on the full-fledged commissioning of SRS eclipse cones from Varian Medical System with limited cone sizes. This study aims at obtaining the beam data required for the commissioning of CCC on a Truebeam linac for 6 MV FFF beam. The study also demonstrates the most comprehensive dosimetric beam parameters of eclipse cone commissioning and validation of experimental data for a 6 MV FFF from Truebeam linac based on the MC approach. Previous studies have validated geometrical modelling and MC simulation of 6 MV FFF from Truebeam linac.<sup>16</sup> The present study is carried out as specific beam data essential for commissioning of the cone dose calculation (CDC) algorithm in eclipse cone treatment planning system (TPS).

## Methods & Materials

The geometrical source modelling of the TrueBeam linac was built using PRIMO version 0.3.64.1814 (<https://www.primoproject.net>) simulation software under fake beam geometry.<sup>17</sup> Here, the study was aimed at MC simulation of CCC and analysing dosimetric characteristics for the SRS eclipse cone manufactured by Varian Medical System (Inc., Palo Alto, CA, USA) for 6 MV FFF Truebeam linac. The CCC acts as a tertiary collimator attached at end below the secondary collimator of linac. All the experimental measurements for CCC were carried out using an EDGE diode detector in a 3D SunScan water scanning system from Sun Nuclear, Melbourne, USA. EDGE detector with a sensitive volume of 0.019 mm<sup>3</sup> and sensitive area of 0.8 × 0.8 mm<sup>2</sup> was used to measure experimental beam data. Besides, the SNC0125c ionization chamber of volume 0.125 cc was used as an intermediate chamber for correcting OFs. The percentage depth dose (PDD), tissue maximum ratios (TMRs), lateral dose profiles (LDPs), and OFs were measured to configure the CDC algorithm for the Varian eclipse cone of diameter 5 mm, 7.5 mm, 10 mm, 12.5 mm, 15 mm, 17.5 mm and validated against MC-simulated beam data. All the experimental measurements were performed to match the commissioning requirements of the eclipse cone beam configuration in TPS. The recommended secondary collimator jaw (X and Y jaw) setting was kept at 5 × 5 cm<sup>2</sup> for beam data measurement of all the cone sizes. The recommendations of TRS-483 were followed during data measurements for the commissioning of SRS cones. The beam data required to commission the CDC algorithm for above mentioned cones were validated against MC using PRIMO.

## PRIMO Monte Carlo simulation

PRIMO is free, non-open source software based on MC general purpose radiation transport code PENELOPE 2011 Salvat et al. for calculation of absorbed dose distribution.<sup>18</sup> PRIMO uses the PENEASY/PENELOPE MC code to simulate Electro-Magnetic (EM) showers in segment-1. PENNELOPE simulates the combined transport of photons, electrons, positrons and their interaction scheme categorized into soft and hard collisions. PENELOPE needs a definite set of simulation parameters under the transport parameter configuration.<sup>19</sup> The default set of parameters used in PRIMO are C1: average angular deflection between consecutive hard collisions, C2: maximum average fractional energy loss between hard collisions, WCC: energy cut-off between hard and soft collisions, WCR: bremsstrahlung energy cut-off, dsMax: maximum allowed step length for charged particles; and E<sub>Abs</sub>: terminal absorption energies. The transport parameters used during the simulation were as, C1 = C2 = 0.1, WCC = 200 KeV, WCR = 50 KeV. The cut-off energies for electron, positron and photon were set at E<sub>abs</sub>(e<sup>-</sup>) = E<sub>abs</sub>(e<sup>+</sup>) = 200 KeV and E<sub>abs</sub>(ph) = 50 KeV. PRIMO simulates the patient's independent and dependent parts of linac performed under segments S1, S2 and S3. Segment S1 allows tallying or producing phase-space file (PSF) at the downstream end of the upper part of linac. Similarly, segment S2 includes PSF tallied or produced at the downstream end of the lower part of linac. At the end, the estimation of absorbed dose distribution in water phantom or CT is included in segment S3. The PSF generated at the end of segment S1 for the upper part of linac during the previous study was used for geometrical source modelling of 6 MV FFF beam from Varian Truebeam linac.<sup>16</sup> Subsequently the simulation of eclipse cones was performed in segment S2. The total numbers of 5 × 10<sup>8</sup> primary particle histories were simulated in S1, which produced a PSF file of 100 gigabytes in size. The simulations of each cone were performed individually during the simulation of segments (S2 + S3) attached at the downstream end of the linac. The initial beam parameters used in modelling of 6 MV FFF beam were initial beam energy, full-width half maxima (FWHM) of energy, FWHM of the focal spot and beam divergence given as 5.85 MeV, 0.05 MeV, 0.8 mm and 0.05 degree, respectively. Absorbed dose distributions were tallied within a slab water phantom of dimension 25 cm × 25 cm × 25 cm with a dose scoring voxel of size  $x = 0.1$  cm,  $y = 0.1$  cm,  $z = 0.1$  cm. The measure of performance of calculations is nothing but computational efficiency ( $\eta$ ), which depends on calculation time (T) and variance ( $\sigma^2$ ). PRIMO introduced the variance reduction technique (VRT) and interaction-forcing factor to increase calculation efficiency. PRIMO recommends Russian roulette splitting as a VRT technique. A higher interaction-forcing factor increases simulation time which consequently reduces the computational efficiency chosen close to 16. The computed tomography (CT) factor recognized as particle splitting in phantom was kept at 100 during MC simulation.

## SRS cone simulation

The SRS cone is a cylindrical tertiary collimator accessory hooked below the secondary collimator. PRIMO allows us to simulate the physical properties of the cone in the segment S2. The distance between the source to bottom of the CCC in a Truebeam linac is fixed at 74 cm. The MC simulations were carried out for a source to CCC distance of 63 cm, physical length of CCC 11 cm and its nominal aperture size at the isocentre. The cones of various diameters ranging from 5 mm to 17.5 mm with an increment of

2.5 mm were simulated. The corresponding PSF generated at the end of the cone was restored in segment S2. PRIMO uses this PSF in its next subsequent segment S3 for final dose computation in water phantom or CT of interest. Table 1 shows the PENELOPE radiation transport parameter used in PRIMO.

**PDD and LDP**

PDD is defined as the absorbed dose at any depth *d* to absorbed dose at the reference depth of dose maxima.<sup>21</sup> The mathematical expression for PDD is written as follows.

$$PDD = \frac{D_d}{D_{ref}} * 100\% \tag{1}$$

where *D<sub>d</sub>* is the dose at any depth and *D<sub>ref</sub>* is the dose at reference depth. *D<sub>ref</sub>* can be the depth of dose maxima. MC simulations of all the cones were performed to obtain simulated PDDs and LDPs in PRIMO. The LDPs are also referred to as off-axis ratios (OARs). Likewise, both sets of PDDs and profiles were measured experimentally using a computer-controlled Radiation 3D-SunScan Field Analyzer (RFA) from Sun Nuclear. These measurements are sensitive to detector position and require detector centring. Therefore, before acquiring the actual depth dose scan centring of the radiation beam axis, the vertical alignment of the cone and detector positioning was verified by using the ray-trace method. This ensures the detector follows the beam centre, which is essential in a small-field depth dose scan. The diameter of a 15 mm cone was used during ray tracing, where LDPs were acquired at depths of 5 cm and 20 cm to determine central beam alignment. The beam central alignment correction was applied for all depth dose scans. In addition, the centring of both profiles was done by central axis correction. The PDD curves were obtained in step-by-step scanning mode with an increment of 1 mm, whereas continuous mode was used to measure dose profiles. All the cone PDDs were simulated and measured at 100 cm SSD and normalized to 100 % at the depth of dose maxima (*D<sub>max</sub>*). Similarly, profiles were measured and simulated at a depth of 5 cm for three different source-to-surface distances (SSD) 80 cm, 90 cm and 100 cm normalized to 100% at the central axis. To analyse the measured PDD and profile curves, they were converted to .dat\* files and imported into the PRIMO workstation. Those sets of data were analysed using the gamma index evaluation tool incorporated in PRIMO as presented by Low et al.<sup>20</sup> Both simulated and measured PDDs and profiles were evaluated based on the gamma analysis index (*γ*) that quantifies the level of agreement or disagreement between measured and MC-simulated curves using gamma-passing criteria of *γ*<sub>2%/1mm</sub> where, (2 % dose difference (% DD) and 1 mm distance to agreement (DTA)) with a minimum passing rate of 95 %. The gamma analysis of dose distribution was performed globally for absolute dose verification. The estimated *γ*<sub>2%/1mm</sub> ≤ 1 and *γ*<sub>2%/1mm</sub> > 1 are considered criteria for passing and failing, respectively.

**Tissue maximum ratio (TMR)**

The TMR is defined as the ratio of the dose rate at a given point in the phantom to the dose rate at the same point for reference depth of dose maxima.<sup>21</sup> The mathematical expression for TMR can be written as,

**Table 1.** Final initial beam parameters used for MC simulation of 6MVFFF nominal beam energy with conical cone collimator for Truebeam linac in PRIMO

Parameters	Description
Processing unit and Processor	Dell precision T7810 Tower Desktop, 32 GB Ram, 2.4 GHz processor
Program/Code/Version	PRIMO/MC-PENELOPE/0.3.64-1814
Transport Parameters	Initial beam energy : 5.85 MeV, FWHM of energy: 0.05 MeV, FWHM of focal size : 0.8 mm, Beam Divergence: 1o C1: Average angular deflection between consecutive hard event C2: Limit maximum average fractional energy loss between consecutive hard event C1 = C2 = 1, WCC: Energy cut-off for bremsstrahlung collision = 200 KeV WCR: Energy cut-off for bremsstrahlung emission = 50KeV Eabs: Absorption emission E <sub>abs</sub> (e <sup>-</sup> ) = E <sub>Abs</sub> (e <sup>+</sup> ) = 200 KeV, E <sub>abs</sub> (Ph) = 50KeV
Variance Reduction Techniques (VRT)	Particle splitting and Russian roulette techniques Forcing factor : 16, CT splitting factor = 100
Histories, Statistical uncertainties (σ), and time (T)	Total number of primary particle histories (Segment: S1) = 1.56 × 10 <sup>8</sup> , Size 100 Gb. Simulation statistical uncertainties ≤ 0.64 % Simulation time for Segment S1:190 Hr., Segment2:10 Hr. to 15 Hr. Simulation efficiency (1/ Δ <sup>2</sup> t) ≈ 356.93x 10 <sup>-8</sup> , where Δ Statistical uncertainty and t is simulation time.

$$TMR = \frac{(D_d)_p}{(D_{max})_p} * 100\% \tag{2}$$

where (*D<sub>d</sub>*)<sub>*p*</sub> is dose at depth *d* at point *p* and (*D<sub>max</sub>*)<sub>*p*</sub> dose at depth of dose maxima at same point *p*. TMR and PPD are interrelated by a classical equation derived by Khan et al.<sup>21</sup>

$$TMR(d, rd) = \frac{P(d, r, SSD)}{100} * \left( \frac{SSD + d}{SSD + d_{max}} \right)^2 * \left( \frac{S_p(r_{dmax})}{S_p(r_d)} \right) \tag{3}$$

where *P* is PDD, *d* is depth, *d<sub>max</sub>* is the reference depth of dose maxima, *r* is the cone field size and *S<sub>p</sub>* is the phantom scatter. The commissioning of cone beam planning needs TMR is a basic requisite for the commissioning of the CDC algorithm in TPS. TMRs were measured directly using a computer-controlled SunScan 3D water phantom (RFA). TMRs were acquired for the range of all cone sizes at a source-detector distance of 100 cm. To reduce spikes in the measurements, TMRs were measured in

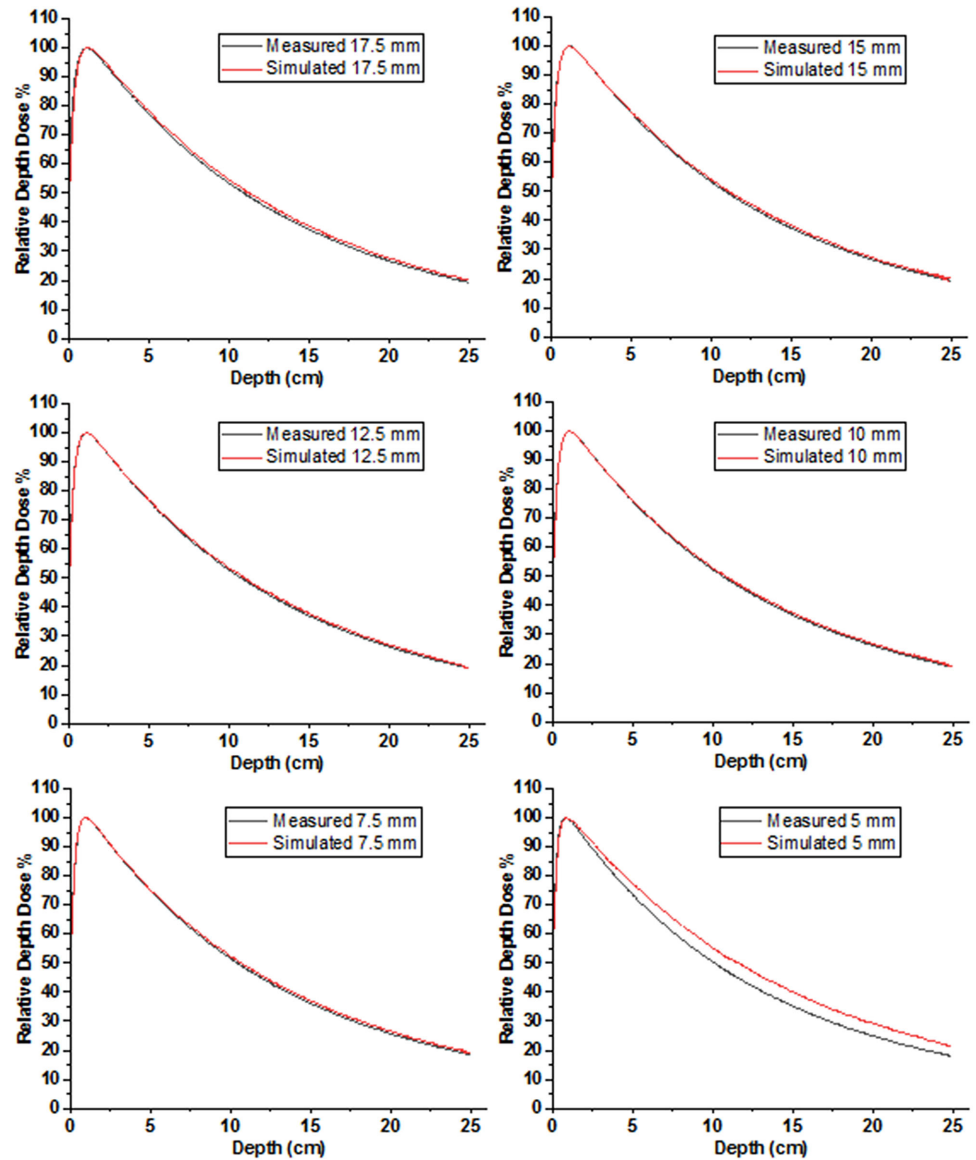


**Figure 1.** Comparison of measured and MC-simulated PDD curves for conical cone collimator of different diameters.

water-draining mode instead of water-filling mode. However, MC-simulated TMRs were indirectly determined by converting MC-simulated PDDs.<sup>22</sup> All the TMR curves were normalized to 100 at  $D_{max}$ , and simulated TMR curves were compared against the measured TMR.

### Cone OFs

The OF is defined as the ratio of output for a given field size to the reference field size at a specific point in the water phantom under maximum scatter conditions.<sup>21</sup> The mathematical expression for the relative OF can be given as,

$$OF = \frac{D(r, d)}{D(r_{ref}, d)} \quad (4)$$

where  $D(r, d)$  is dose for a field at depth  $d$  and  $D(r_{ref}, d)$  is dose for reference field at same depth  $d$ . The OFs were measured at a depth of 5 cm for source-to-phantom distance (SPD) at 95 cm and source-to-axis distance (SAD) at 100 cm in an isocentric setup.

Similarly, OFs were estimated for the same field geometry arrangement using the MC simulation approach in PRIMO. All the measured OFs were corrected for their limitations in small-field dosimetry. For this, the small-field detector (SFD) was cross-calibrated using the cylindrical chamber SNC0125c at an intermediate open field of  $3 \times 3 \text{ cm}^2$  known as intermediate daisy-chain method.<sup>23</sup> OFs were normalized for an open reference field size of  $10 \times 10 \text{ cm}^2$ . The corrected OFs were determined as follows,

$$OF_{Corr.} = \frac{SFD_{(Cone)}}{SFD_{(3 \times 3)}} * \frac{CC0125_{c(3 \times 3)}}{CC0125_{c(10 \times 10)}} \quad (5)$$

where  $SFD_{(Cone)}$  is EDGE diode reading for various cone sizes.  $SFD_{(3 \times 3)}$  is for diode open field reading. Similarly,  $CC0125_{c(3 \times 3)}$  and  $CC0125_{c(10 \times 10)}$  are the reading for open fields using SNC0125c. The dose output for all the cones and the reference field size were determined using MC simulation. PRIMO-simulated OFs were validated against experimentally measured OFs.



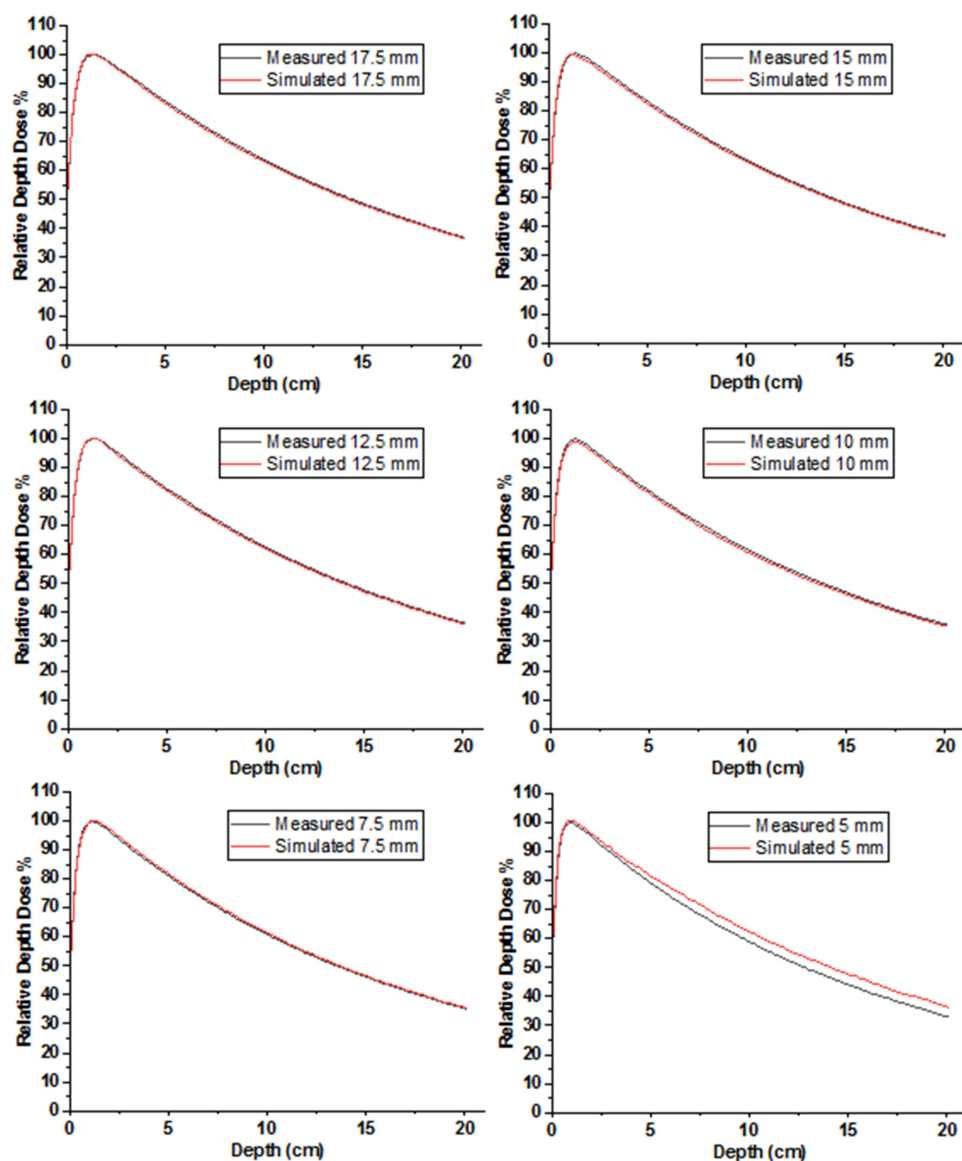


**Figure 2.** Comparison of measured and MC-simulated TMR curves for conical cone collimator of different diameters.

**CDC algorithm and absolute dose measurement**

The CDC algorithm has been employed in eclipse cone planning to calculate the dose for stereotactic cone collimator in the treatment of SRS. CDC uses TMR, OAR and cone OFs to determine dose at any point within the volume. CDC calculates the dose at any arbitrary point is given by,

$$D(r, d, SSD, S) = MU * DR_{ref} * OF_{TMR}(s) * TMR(d, s) * \left( \frac{SAD}{SSD + d} \right)^2 * OAR(r, s) \tag{6}$$

where

$D(r, d, SSD, S)$  = Dose at location of interest,  $MU$  = Delivered monitor unit,

$DR_{ref}$  = Reference Dose rate,  $OF$  = Output Factors,

$TMR(d, s)$  = Tissue Maximum Ratio,  $OAR(r, s)$  = Off-Axis Ratio,

$r$  is off-axis distance,  $d$  is the depth of point of interest along the central axis, and  $S$  is nominal diameter of the conical collimator. However, the CDC has its limitations such as the approximation of an arc beam as a static beam, the absence of backscatter near the cavities and exit of the beam, ignoring tissue inhomogeneity and obliquity of beam entry. CDC requires absolute dose measurement in beam configurations measured at a depth of 5 cm for a reference field size of  $10 \times 10 \text{ cm}^2$  and SPD 95 cm. The absolute dose measurement was simulated under the same reference geometry setting in PRIMO.

**Results**

The experimental beam data acquired for various cones of 5 mm, 7.5 mm, 10 mm, 12.5 mm, 15 mm and 17.5 mm were validated using MC. The initial beam parameters obtained iteratively that truly exhibit characteristics of our existing Truebeam linac are shown in Table 1. The experimentally measured and MC absolute dose obtained at a depth of 5 cm for SSD 95 cm were matched within 0.5 % showing excellent agreement. The maximum

**Table 2.** MC-simulated PDD and TMR versus experimentally measured PDD and TMR for cones of different sizes

Cone size (mm)	PDD								
	PDD at 10cm depth			PDD at 20cm depth			Range at 50 % dose (cm)		
	Measured	Simulated	% Difference	Measured	Simulated	% Difference	Measured	Simulated	% Difference
5	50.55	52.60	-4.05	24.99	26.87	-7.52	10.13	10.69	-5.52
7.5	51.70	52.45	-1.45	25.79	26.54	-2.90	10.46	10.70	-2.22
10	52.41	52.95	-1.01	26.27	26.91	-2.37	10.64	10.84	-1.84
12.5	52.91	53.50	-1.11	26.50	27.13	-2.37	10.80	11.04	-2.22
15	53.42	54.08	-1.23	26.70	27.32	-2.32	10.91	11.16	-2.29
17.5	53.51	54.12	-1.13	26.69	27.42	-2.73	10.96	11.25	-2.64
Cone size (mm)	TMR								
	*TMR at 10cm depth			*TMR at 20 cm depth			Range at 50 % dose (cm)		
	Measured	Simulated	% Difference	Measured	Simulated	% Difference	Measured	Simulated	% Difference
5	58.91	61.29	-4.04	33.13	35.46	-7.03	12.80	13.47	-5.23
7.5	60.97	61.67	-1.14	35.37	36.35	-2.77	13.50	13.78	-2.07
10	61.68	60.91	1.24	35.98	35.45	1.47	13.85	13.75	0.72
12.5	62.68	62.03	1.03	36.52	36.01	1.39	14.15	14.02	0.91
15	63.16	62.56	0.94	37.23	37.02	0.56	14.35	14.25	0.69
17.5	63.79	63.52	0.42	37.22	37.11	0.29	14.50	14.50	0.0

Note: All the \*TMR values are multiplied by 100.

**Table 3.** Gamma analysis of measured and MC-simulated PDD curves for different cone sizes

Cone size (mm)	Measured Dmax (cm)	Simulated Dmax (cm)	Average gamma index before maximum	Average gamma index after maximum	Percentage of points passing criteria at (2%, 1mm)	% Dose difference (DD) at 10 cm	Distance to agreement (DTA) mm at 10 cm	Gamma index at 10 cm
5	0.84	0.84	0.22	0.50	98.78	-4.05	0.85	0.51
7.5	0.96	1.04	0.18	0.32	99.15	-1.45	0.63	0.33
10	1.05	1.05	0.19	0.21	99.52	-1.01	0.22	0.27
12.5	1.16	1.06	0.24	0.31	99.67	-1.11	0.23	0.33
15	1.15	1.05	0.25	0.30	99.62	-1.23	0.22	0.41
17.5	1.04	1.07	0.32	0.49	99.75	-1.13	0.35	0.37

statistical uncertainties during the MC simulation estimated at the end of segment S3 were found to be 0.64%.

### MC validation of PDD & TMR

Figures 1 and 2 compare the measured and MC-simulated PDDs and TMRs curves for conical cone beams of various cone sizes, respectively. The misalignment of the cone and detector along the central axis was found to be  $0.03^\circ$  to the extent of 20 cm depth. This central axis offset error was corrected using the ray-trace method for all depth dose scans. Table 2 summarizes the depth dose values for measured and simulated PDDs and TMRs. Both sets of measured and simulated PDD and TMR curves for all the cones are nicely superimposed on each other except for the smallest cone of 5 mm diameter shown in Figs. 1 and 2, respectively. The result shows the maximum deviation between measured and simulated PDDs or TMRs were within 3% except

for cone of 5 mm diameter. The difference between measured and simulated PDDs or TMRs at depths of 10 cm, 20 cm and at range of 50 % dose was substantially higher for diameters of smaller cone sizes. The maximum deviation in PDDs and TMRs at depths of 10 cm, 20 cm and at range of 50% dose was found 4.05 %, 7.52 %, 5.52 % and 4.04 %, 7.03 %, 5.23 %, respectively, for the cone of 5 mm diameter. Close agreements were seen between values of measured and simulated depth of dose maxima ( $d_{max}$ ) and ratio of PDDs at 20 cm and 10 cm depth ( $PDD_{20/10}$ ). The differences between measured and simulated values of  $d_{max}$  were found below 0.1 mm as shown in Table 3. The ratio of  $PDD_{20/10}$  for the measured and its corresponding simulated PDDs were found  $0.49 \pm 0.01$  and  $0.5 \pm 0.01$  over the range of dimensions for various cone sizes. The result of gamma analysis shows close agreement between the dose distribution obtained for measured and simulated depth dose curves. The average gamma index before and after dose maxima were found  $\bar{\gamma}_{2\%/1mm} \leq 1$  with a

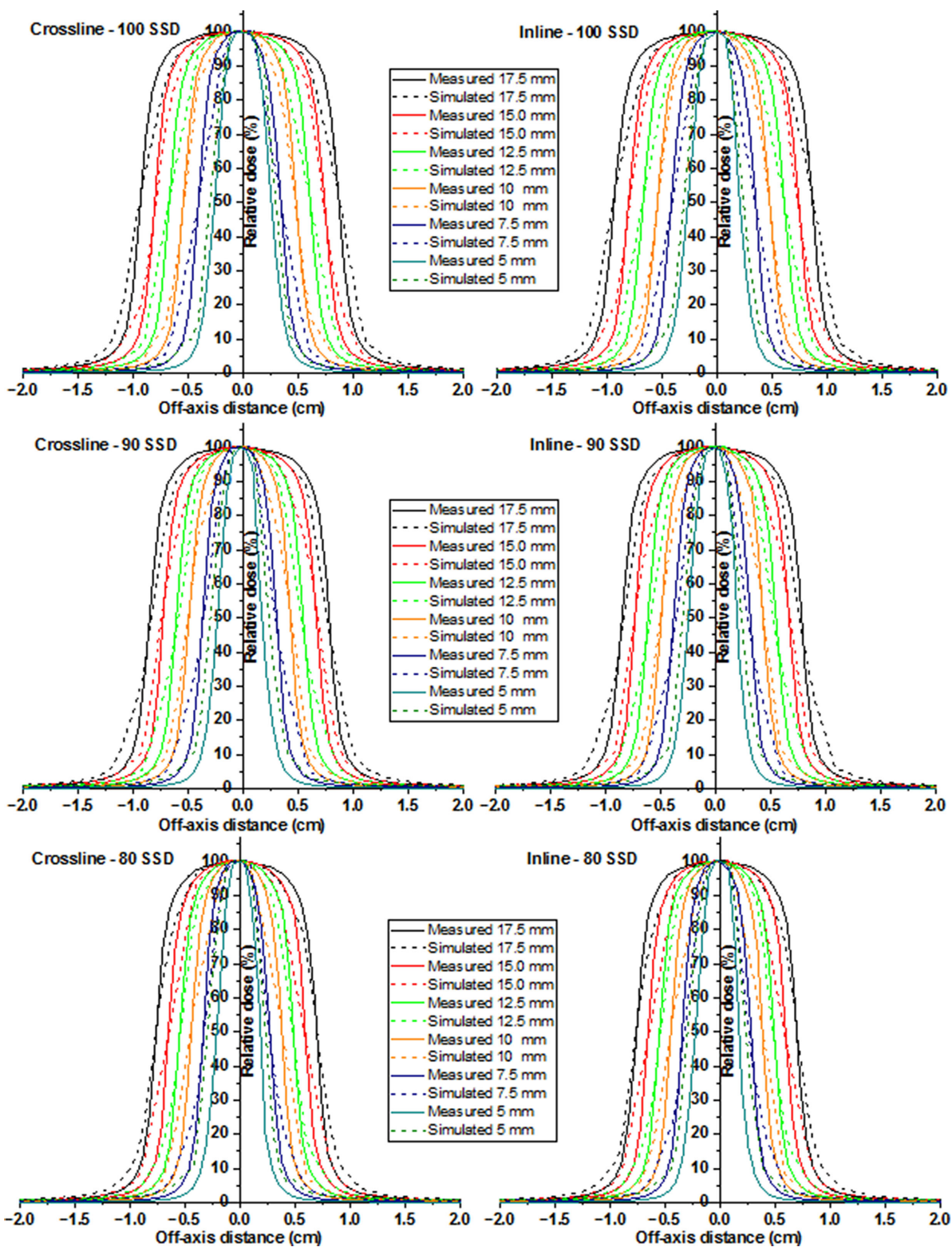


**Figure 3.** Comparison of measured and MC-simulated lateral dose profiles for conical cone collimator of different diameters.

minimum percentage of point passing  $\geq 98.78\%$  for all the cones. The gamma analysis results for  $\gamma_{2\%/1\text{mm}}$  also show maximum deviation in % DD, and DTA were observed for 5 mm cone at a depth of 10 cm shown in Table 3.

#### MC validation of LDPs

The comparisons of measured and MC-simulated LDPs obtained for the diameter of different conical cones are shown in Fig. 3. This shows LDPs (cross-line and in-line) measured at a depth of 5 cm

**Table 4.** FWHM of simulated and measured depth dose profiles at 5 cm depth for SSD 100 cm

Cone size (mm)	Transverse profile							
	Left off-axis distance at 50 % dose (cm)		Right off-axis distance at 50 % dose (cm)		FWHM of Cone (cm)		% Dose at values of FWHM	
	Measured	Calculated	Measured	Calculated	Measured	Calculated	Measured	Calculated
5	-0.23	-0.27	0.23	0.27	0.5	0.5	3.38	9.15
7.5	-0.37	-0.37	0.37	0.37	0.74	0.74	2.24	4.39
10	-0.51	-0.51	0.51	0.51	1.02	1.02	1.55	2.74
12.5	-0.64	-0.64	0.64	0.64	1.28	1.28	1.32	2.06
15	-0.77	-0.76	0.77	0.76	1.54	1.52	1.25	1.81
17.5	-0.89	-0.90	0.89	0.90	1.78	1.80	1.30	1.60
Cone size (mm)	Longitudinal profile							
	Left off-axis distance at 50 % dose (cm)		Right off-axis distance at 50 % dose (cm)		FWHM of Cone (cm)		% Dose at values of FWHM	
	Measured	Calculated	Measured	Calculated	Measured	Calculated	Measured	Calculated
5	-0.24	-0.27	0.24	0.27	0.5	0.5	3.49	9.11
7.5	-0.38	-0.37	0.38	0.37	0.74	0.74	2.17	4.34
10	-0.51	-0.51	0.51	0.51	1.02	1.02	1.47	2.70
12.5	-0.64	-0.64	0.64	0.64	1.28	1.28	1.27	2.09
15	-0.77	-0.76	0.77	0.76	1.54	1.52	1.20	1.80
17.5	-0.89	-0.90	0.89	0.90	1.78	1.80	1.31	1.64

**Table 5.** Comparison of measured and MC-simulated depth dose profiles at 5 cm depth for SSD 100 cm

Cone size (mm)	Transverse profile					
	Deviation at 80 % dose (cm)		Deviation at 50 % dose (cm)		Deviation at 20 % dose (cm)	
	Left side % DD/ Δ(mm)	Right side % DD/ Δ(mm)	Left side % DD/ Δ(mm)	Right side % DD/ Δ(mm)	Left side % DD/ Δ(mm)	Right side % DD/ Δ(mm)
5	-5.12/0.24	-8.58/-0.30	-14.29/0.42	-14.35/-0.42	-13.76/0.41	-15.21/-0.66
7.5	14.24/-0.70	12.83/0.63	-0.11/-0.01	0.18/0.01	-16.31/0.94	-16.10/-0.94
10	7.50/-0.27	10.95/0.53	2.38/-0.09	2.46/0.09	-7.13/0.39	-4.68/-0.21
12.5	13.72/-0.83	14.25/0.87	-0.40/0.02	-0.27/-0.02	-14.60/0.80	-14.28/-0.79
15	11.31/-0.64	7.92/0.36	2.51/-0.10	2.35/0.10	-6.67/0.41	-8.21/-0.57
17.5	13.16/-0.93	13.33/0.93	-1.36/0.08	-1.29/-0.08	-13.87/0.73	-14.40/-0.76
Cone size (mm)	Longitudinal profile					
	Deviation at 80 % dose		Deviation at 50 % dose		Deviation at 20 % dose	
	Left side % DD/ Δ(mm)	Right side % DD/ Δ(mm)	Left side % DD/ Δ(mm)	Right side % DD/ Δ(mm)	Left side % DD/ Δ(mm)	Right side % DD/ Δ(mm)
5	-4.57/0.26	-7.19/-0.23	-11.76/0.35	-11.83/-0.35	-10.97/0.37	-12.71/-0.55
7.5	14.15/-0.70	14.28/0.71	1.50/-0.09	1.65/0.09	-13.45/0.78	-14.56/-0.84
10	6.86/-0.32	9.07/0.48	1.27/-0.05	1.42/0.05	-7.29/0.43	-5.27/-0.19
12.5	14.52/-0.88	13.83/0.84	-0.31/0.02	-0.33/-0.02	-14.65/0.80	-13.39/-0.78
15	8.88/-0.49	7.73/0.33	2.76/-0.11	2.77/0.11	-6.13/0.30	-8.17/-0.49
17.5	12.52/-0.90	12.34/0.89	-1.78/0.10	-1.75/-0.1	-13.33/0.71	-15.39/-0.80

Note: Lt. = Left side % dose difference (% DD), Rt. = Right side % dose difference (% DD), Δ = Relative Distance (mm).

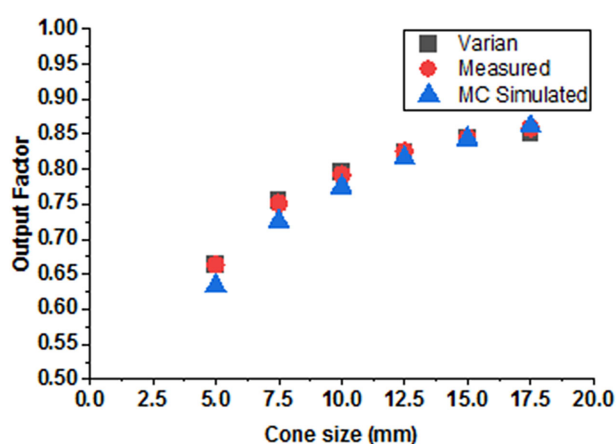


**Table 6.** Gamma analysis of measured and MC-simulated depth dose profiles at 5 cm depth and 100 cm SSD for various cone sizes

Cone size (mm)	Average gamma index inside the field		Average gamma index outside the field		Average gamma index in penumbra region		Percentage of points passing criteria (2%, 1mm)	
	Transverse	Longitudinal	Transverse	Longitudinal	Transverse	Longitudinal	Transverse	Longitudinal
5	0.53	0.48	0.19	0.18	0.68	0.58	97.1	98.0
7.5	0.38	0.38	0.14	0.14	0.57	0.59	98.8	98.7
10	0.35	0.39	0.12	0.12	0.53	0.61	99.0	99.1
12.5	0.38	0.39	0.12	0.13	0.52	0.55	99.3	99.5
15	0.36	0.34	0.12	0.11	0.54	0.59	99.3	99.5
17.5	0.37	0.34	0.11	0.11	0.63	0.53	99.5	99.6

**Table 7.** Comparison of measured and MC estimated output factors

Cone size (mm)	Varian Golden beam data OFs	Measured OFs (EDGE <sub>Corr.</sub> )	Simulated OFs (PRIMO)	% Deviation
5	0.664	0.663	0.633	-4.78
7.5	0.755	0.757	0.725	-3.63
10	0.795	0.792	0.775	-2.25
12.5	0.824	0.825	0.815	-1.21
15	0.845	0.845	0.843	-0.14
17.5	0.852	0.859	0.861	0.26

**Figure 4.** Comparison of measured and MC-simulated output factors for conical cone collimator of different diameters.

for cones of different diameters at three different SSDs. The values of FWHM represent the size of the conical cone estimated from measured, and MC-simulated profiles are within  $\pm 0.2$  mm summarized in Table 4. However, percentage doses obtained at values of FWHM exhibit good agreement between measured and MC-calculated doses below 3 % for the diameter of all cones except for the 5 mm cone. Table 5 summarizes the results for variation of measured and MC-simulated percentage dose profiles compared at 80 %, 50 % and 20 % doses for depth of 5 cm and SSD 100 cm. This deviation in percentage dose difference (% DD) and relative distances (RD) were found substantially higher in the penumbra region around 80 % and 20 % dose profiles for all cones. The

greatest difference between measured and MC values of % DD or RDs in the penumbra region of dose profiles over all the cones was found below  $\pm 15.5$  % and 1 mm, respectively. However, % DDs and RDs in the region of 50 % dose profiles (central region) were found below  $\pm 2.5$  % and 0.11 mm except for 5 mm cone. The penumbra region in the measured dose profiles was found to have a steeper descent compared to MC-simulated profiles. The penumbra for measured and MC dose profiles varies from 1-to-2.5 mm and 1.5-to-3.5 mm over all cone sizes, respectively. The maximum disagreement between the penumbra of measured and MC dose profiles was found below 1.5 mm over all the cone sizes. Table 6 summarized gamma-passing results for measured, and MC LDPs acquired at a depth of 5 cm and SSD 100 cm were analysed using  $\Upsilon_{2\%/1\text{mm}}$  criteria. The maximum average gamma index inside, outside and in the penumbra regions, was within 0.51, 0.18 and 0.68 with a minimum percentage of  $\Upsilon_{2\%/1\text{mm}}$  passing rate  $\geq 97.6$  % respectively, for both transverse and longitudinal profiles. This indicates overall agreement between measured and MC dose profiles.

### Cone OFs

Table 7 summarizes measured and simulated OFs for circular fields of various cone sizes. The OFs measured using an EDGE diode detector corrected with an intermediate field were compared against the MC-simulated OFs. OFs are functions of cone diameters, which increase with the cone size. The variation of measured and simulated OFs together with Varian recommended OFs as a function of cone diameter are plotted in Fig. 4. This shows the difference between measured and MC-simulated OFs is consistently increasing as size of the cone reduces. The measured

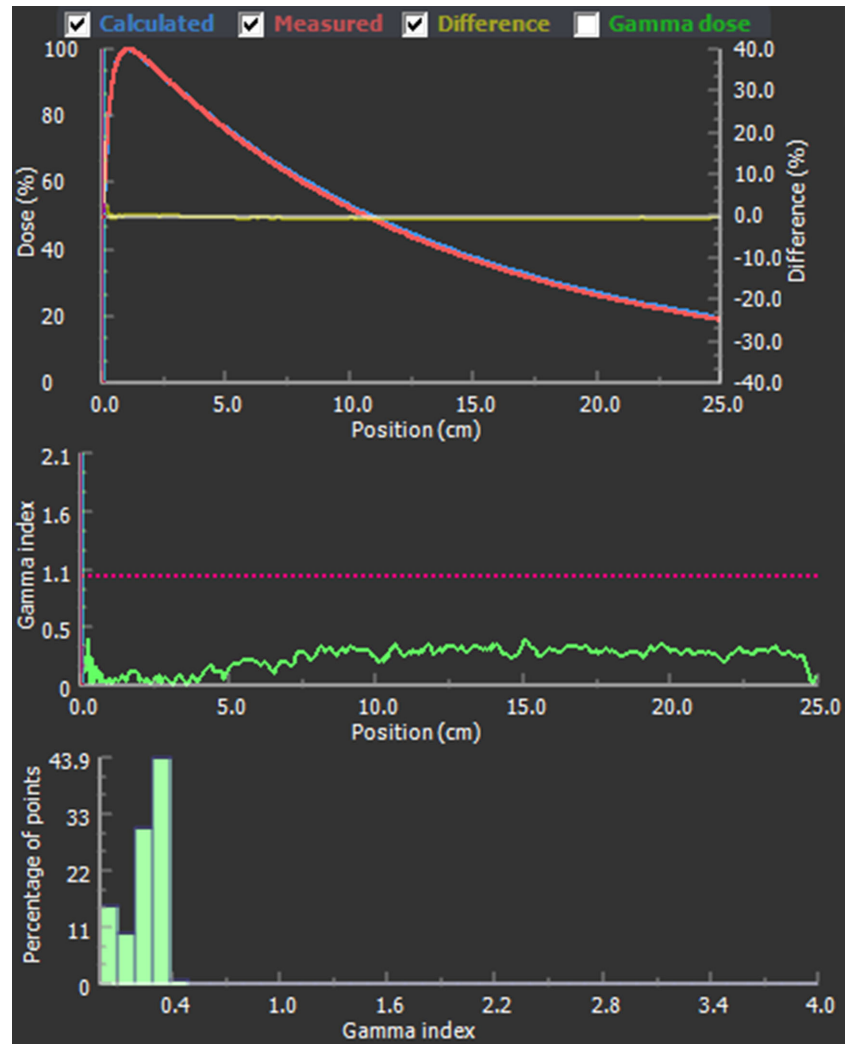


**Figure 5.** Comparison of measured PDD relative to MC. This also illustrates variation of gamma index along the depth of PDD and percentage of gamma passing.

OFs are consistently larger than the MC-simulated using PRIMO. The Varian OFs agreed very well with the measured OFs. However, simulated OFs showed more deviation than measured ones as the cone size gets smaller. The maximum deviation of 4.78 % was observed between simulated and measured OFs for the smallest cone of 5 mm diameter. These differences between OFs for cones greater than 10 mm were found to be below 3 %. The OFs for cone diameters of 15 mm and higher are perfectly matched below 0.5%.

### Discussion

The MC model of the Varian conical cone for the 6 MV FFF beam from Truebeam linac was presented and its dosimetric validation of SRS eclipse cone beam data (PDDs, TMRs, LDP and OFs) has been performed using MC simulation. The measured and simulated PDDs or TMRs are in good agreement with each other except for a cone of 5 mm diameter. The PDDs, TMRs and  $D_{\max}$  are functions of cone size that increase as cone size increases as would be expected.<sup>24</sup> Both the measured and MC PDDs or TMRs curves for cones of 10 mm or higher are closely overlaid within 1.5 %. However, significant divergence is seen below 10 mm for 7.5 mm and 5 mm cones at higher depth. Smaller cones have a greater tendency to be misaligned with the beam's central axis and detector. A slight misalignment of the cone and detector central

axis could result in a larger dose variation. From Figs. 1 and 2 one can appreciate that measured PDD curves exhibit slightly low doses, which could be the result of the small electron range in diode material and volume averaging response of diode detector at the small field for low-energy photons relative to MC.<sup>7</sup> The experimentally measured TMRs were compared against TMRs converted from MC PDDs, because PRIMO does not provide MC-simulated TMRs directly. Both measured and MC TMR curves are nicely superimposed on each other except for the 5 mm cone. Diode detectors have their own issues associated with dose rate, energy and directional dependence. In addition, as the size of the beam gets smaller and narrower, electronic equilibrium tends to decrease. The contributions of those effects are primarily observed in the smallest cone of 5 mm diameter as can be seen in Figs. 1 and 2. The accuracy of simulated PDDs or profiles also depends on the number of particle histories and typical voxel size. As PENELOPE allows only a fixed number of voxel  $10^8$  in S3 simulations, it limits the size of voxel results in averaging of dose. The maximum statistical uncertainties in the measurement were 0.64 %.

The comparisons of measured and MC-simulated LDPs also referred as OARs are the function of off-axis distance for a cone of different diameters at different SSD as shown in Fig. 3. This also demonstrates that the widening of the profile increases with an increase in SSD caused by beam divergence. The resultant

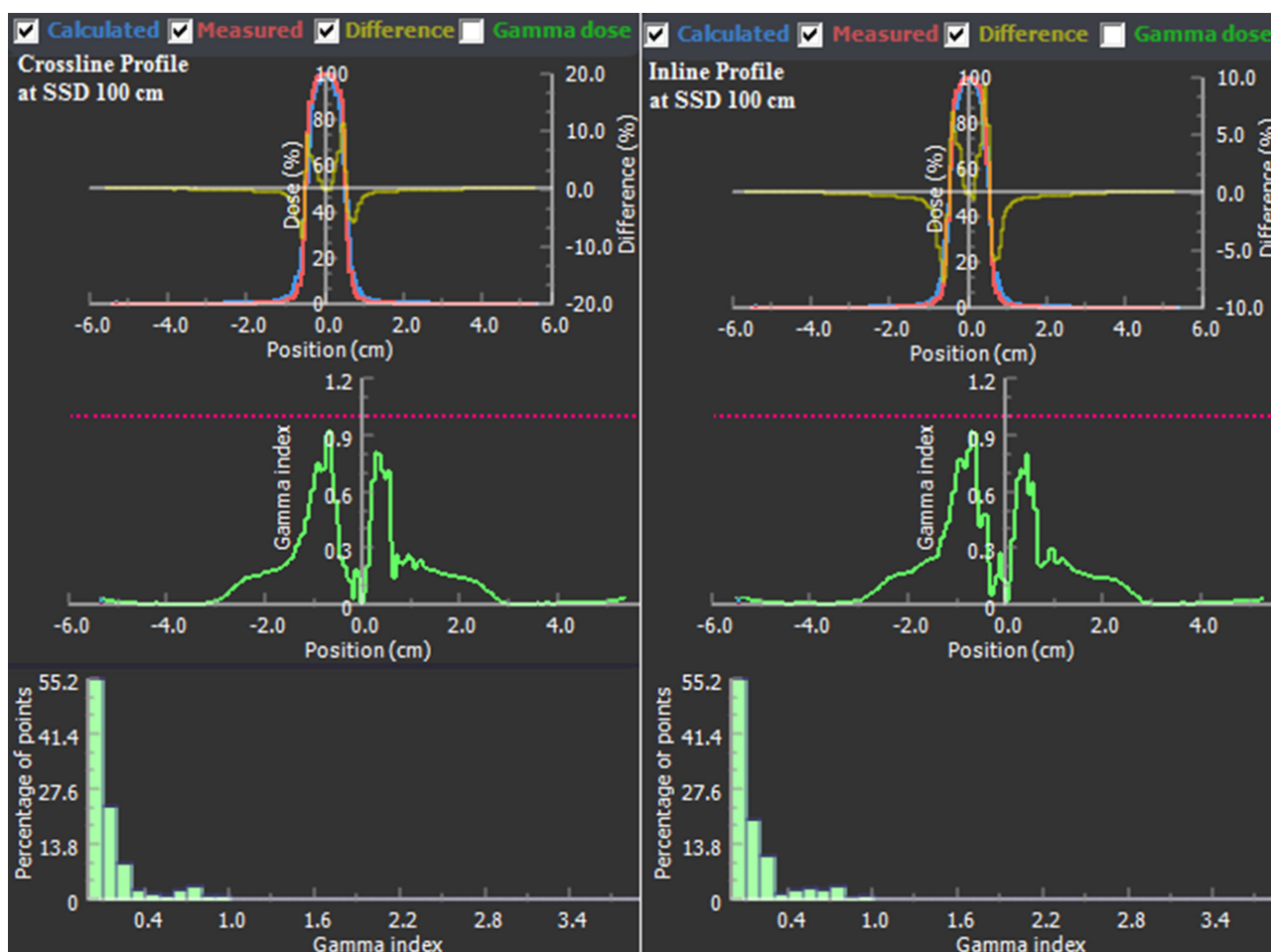


**Figure 6.** Comparison of measured lateral dose profile relative to MC. This also illustrates variation of percentage dose and gamma index with position for 10 mm cone size.

average gamma index and percentage of gamma passing for the comparison of measured and MC profiles summarized in Table 7 indicate close agreements between them. The measured FWHM is a characteristic of the physical dimension of the cone that agrees with MC's estimated FWHM within  $\pm 0.2$  mm. The disagreement between the measured and MC dose at the point of FWHM was found below 3% except for the 5 mm cone. The difference between measured and MC doses at FWHM found to be increase as the size of the cone decreased. The FWHM of the beam profile lies in the high dose gradient region which makes it highly sensitive to detector position. The lateral distance between 80% and 20% of dose profiles gives penumbra indicating steepness of descent of the curves increases with cone size can be appreciated from Fig. 3. The doses in the penumbra region around 80% of dose profiles are substantially higher in experimentally measured profiles relative to MC. However, measured doses around 20% region and beyond are found to be significantly lower compared to MC. The response function of the diode detector depends on the sensitive region of the detector, and EDGE diodes have a sensitive region of 0.8 mm. The region of 80% dose profile that slightly diverges from the centre relative to the MC profile could be due to over-response of the detector for low-energy photons within the field. Its prominent impact could have been seen in the 5 mm cone, where the measured profile completely encompassed within MC profile. However, dose at 20% of the profile little converges towards the centre relative to MC. This might be the effect of the small

electron range and insufficiency of the diode detector to account for transmission of the beam due to the bottom end of the cone in region 20% of dose profile and beyond it. However, MC takes into account dose precisely in the low-dose region beyond the penumbra and the range of electrons outside the field. In addition, dose along LDPs are greatly influenced by dose averaging effects due to the number of voxels that are accommodated within the radiation field of the cone.

The measured OFs are in good agreement with data reported by Varian within 1% shown in Fig. 4. The measured and MC-simulated OFs exhibit good agreement for cone sizes 10 mm and above. However, considerable deviations were observed below 10 mm for 7.5 mm and 5 mm cones. The agreement between measured and MC OFs for the largest cone of 17.5 mm and the smallest cone of 5 mm were found 0.26% and 4.78%, respectively. The agreement was poorer for the smallest cone size of 5 mm diameter. The diode detectors have limitations caused by volume averaging and water nonequivalence could predominantly affect measured OFs. Therefore, OFs measured with a diode detector need to be corrected to minimize effect due to its limitations. The use of the intermediate Daisy-chain method minimized the difference between measured and MC OFs.<sup>23</sup> However, the response of the diode detectors may be directional and energy-dependent which could lead to dosimetric uncertainties up to  $\pm 15\%$  are beyond the scope of correction of our work.<sup>25</sup>

Gamma analysis helps in the characterization of dosimetric data such as PDD and profile. Gamma analysis facilitates the quantitative evaluation of dose distribution presented by Low et al.<sup>20</sup> The maximum value of  $\Upsilon_{2\%/1\text{mm}}$  corresponding to the maximum dose difference is below 0.5 and 0.9 for PDDs and profiles of all the cones, respectively. The values of  $\Upsilon_{2\%/1\text{mm}}$  in all regions of PDDs or profiles are below 1. Both % DD and DTA lie below the passing criteria for PDD. However, for profile DDs are higher in the dose gradient region whereas DTA are well within the limit. This established good agreements between measured and MC PDDs or profiles for all cones except for the 5 mm cone. Figures 5 and 6 illustrate the comparison of measured and simulated PDD and lateral profile distribution with gamma index for diameter of 10 mm cone, respectively.

## Conclusion

The MC model of eclipse cone for 6 MV FFF beam from a Truebeam linac was presented in PRIMO. The study presents the MC validation of experimental beam data required for the commissioning of CDC algorithm used in eclipse TPS. An overall good agreement was found between experimentally measured and MC-simulated data. It was also found that the degree of agreement subsides, as the cone size gets smaller below 10 mm. The dosimetry dataset obtained in this study validated using MC model may be used to benchmark beam data measured for commissioning of SRS cone for the eclipse planning system.

**Acknowledgements.** The author would like to thank to people who drove him for their continuous assistance and encouragement and made this work possible.

**Financial support.** No financial support or funding provided for this study.

**Competing interests.** Authors declare no conflict of interest.

## References

1. Tuleasca C, Regis J, Sahgal A, et al. Stereotactic radiosurgery for trigeminal neuralgia: a systematic review. *J Neurol Surg* 2019; 130: 733–757.
2. Gevaert T, Levivier M, Lacornerie T, et al. Dosimetric comparison of different treatment modalities for stereotactic radiosurgery of arteriovenous malformations and acoustic neuromas. *Radiother Oncol* 2013; 106: 192–197. <https://doi.org/10.1016/j.radonc.2012.07.002>.
3. Benedict S H, Yenice K M, Followill D, et al. Stereotactic body radiation therapy: the report of AAPM Task Group 101. *Med Phys* 2010; 37 (8): 4078–4101. <https://doi.org/10.1118/1.3438081>
4. ICRU. Prescribing, recording and reporting of stereotactic treatments with small photon beams (ICRU 91). *J ICRU* 2014; 14 (1): 1–2. <https://doi.org/10.1093/jicru/ndw036>
5. Rogers D W O, Faddegon B A, Ding G X, Ma C M, We J, Mackie T R. BEAM: a Monte Carlo code to simulate radiotherapy treatment units. *Med Phys* 1995; 22 (5), 503–524. <https://doi.org/10.1118/1.597552>
6. Cheng J Y, Ning H, Arora B C, Zhuge Y, Miller R W. Output factor comparison of Monte Carlo and measurement for Varian TrueBeam 6 MV and 10 MV flattening filter-free stereotactic radiosurgery system. *J Appl Clin Med Phys* 2016; 17 (3): 100–110. <https://doi.org/10.1120/jacmp.v17i3.5956>
7. Khelashvili G, Chu J, Diaz A, Turian J. Dosimetric characteristics of the small diameter BrainLabTM cones used for stereotactic radiosurgery. *J Appl Clin Med Phys* 2012; 13 (1): 4–13. <https://doi.org/10.1120/jacmp.v13i1.3610>
8. Garnier N, Amblard R, Villeneuve R, et al. Detectors assessment for stereotactic radiosurgery with cones. *J Appl Clin Med Phys* 2018; 19 (6): 88–98. <https://doi.org/10.1002/acm2.12449>
9. Huang T-A P, Morales J E, Butson E, Johnson A, Butson M, Hill R A. A novel extrapolation method using OSL detectors for very small field output factor measurement for stereotactic radiosurgery. *Phys Eng Sci Med* 2020; 43 (2): 593–599. <https://doi.org/10.1007/s13246-020-00859-2>
10. Belec J, Patrocinio H, Verhaegen F. Development of a Monte Carlo model for the Brainlab microMLC. *Phys Med Biol* 2005; 50 (5): 787–799. <https://doi.org/10.1088/0031-9155/50/5/005>
11. Chaves A, Lopes M C, Alves C C, Oliveira C, Peralta L, Rodrigues P, Trindade A. Basic dosimetry of radiosurgery narrow beams using Monte Carlo simulations: a detailed study of depth of maximum dose. *Med Phys* 2003; 30 (11): 2904–2911. <https://doi.org/10.1118/1.1618031>
12. Chaves A, Lopes M C, Alves C C, Oliveira C, Peralta L, Rodrigues P, Trindade A. A Monte Carlo multiple source model applied to radiosurgery narrow photon beams. *Med Phys* 2004; 31 (8): 2192–2204. <https://doi.org/10.1118/1.1766419>
13. Morales J E, Crowe S B, Hill R, Freeman N, Trapp J V. Dosimetry of cone-defined stereotactic radiosurgery fields with a commercial synthetic diamond detector. *Med Phys* 2014; 41 (11): 111702. <https://doi.org/10.1118/1.4895827>
14. Hermida-López M, Sánchez-Artuñedo D, Rodríguez M, Brualla L. Monte Carlo simulation of conical collimators for stereotactic radiosurgery with a 6 MV flattening-filter-free photon beam. *Med Phys* 2021; 48 (6): 3160–3171. <https://doi.org/10.1002/mp.14837>
15. Wiant D B, Terrell J A, Maurer J M, Yount C L, Sintay B J. Commissioning and validation of BrainLAB cones for 6X FFF and 10X FFF beams on a Varian TrueBeam STx. *J Appl Clin Med Phys* 2013; 14 (6): 4493. <https://doi.org/10.1120/jacmp.v14i6.4493>
16. Shende R, Dhoble S J, Gupta G. Geometrical source modeling of 6MV flattening-filter-free (FFF) beam from TrueBeam linear accelerator and its commissioning validation using Monte Carlo simulation approach for radiotherapy. *Radiat Phys Chem* 2022; 199: 110339. <https://doi.org/10.1016/j.radphyschem.2022.110339>
17. Rodríguez M, Sempau J, Brualla L. PRIMO: A graphical environment for the Monte Carlo simulation of Varian and Elekta linacs. *Strahlenther Onkol* 2013; 189 (10): 881–886. <https://doi.org/10.1007/s00066-013-0415-1>
18. Salvat F, Fernandez-Varea J M, Sempau J. PENELOPE—A Code System for Monte Carlo Simulation of Electron and Photon Transport: OECD Nuclear Energy Agency; 2011.
19. Brualla L, Rodríguez M, Sempau J. Primo User's manual version 0.3. 1.1600. *Strahlenklinik, Hufelandstrasse*, 55, 2018.
20. Low D A, Harms W B, Mutic S, Purdy J A. A technique for the quantitative evaluation of dose distributions. *Med Phys* 1998; 25 (5): 656–661. <https://doi.org/10.1118/1.598248>
21. Khan F M. *The Physics of Radiation Therapy*. Baltimore, MD: Williams and Wilkins; 1994.
22. Battum L J van, Essers M, Storchi P R M. Conversion of measured percentage depth dose to tissue maximum ratio values in stereotactic radiotherapy. *Phys Med Biol* 2002; 47 (18): 3289–3300. <https://doi.org/10.1088/0031-9155/47/18/302>
23. IAEA and AAPM, TRS-483. Dosimetry of Small Static Fields Used in External Beam Radiotherapy. 2017.
24. Palta J R. Dosimetric characteristics of clinical photon beams. In D W Rogers & J E Cygler (Eds.), *Clinical dosimetry measurements in radiotherapy*. Proceedings of the American Association of Physicists in Medicine Summer School (pp. 323–362): Colorado College. Medical Physics Publishing; 2009.
25. Saini A S, Zhu T C. Energy dependence of commercially available diode detectors for in-vivo dosimetry. *Med Phys* 2007; 34 (5): 1704–1711. <https://doi.org/10.1118/1.2719365>